Four layer multi-omics reveals molecular responses to aneuploidy in *Leishmania*

Cuypers B.[1,2], Meysman P.[2], Erb I.[3], Bittremieux W.[4], Valkenborg D.[5,6], Baggerman G.[6,7], Mertens I.[6,7], Shyam Sundar[8], Basudha Khanal[9], Notredame C.[3], Dujardin, J-C.[1,10#], Domagalska M.A.[1*#], Laukens K.[2*#]

1. Molecular Parasitology Unit, Department of Biomedical Sciences, Institute of Tropical Medicine, Antwerp, Belgium.

2. Adrem Data Lab, Department of Computer Science, University of Antwerp, Antwerp, Belgium.

3. Centre for Genomic Regulation (CRG), The Barcelona Centre of Science and Technology, Barcelona, Spain.

4. Skaggs School of Pharmacy and Pharmaceutical Sciences, University of California San Diego, La Jolla, CA 92093, USA.

5. Center for Statistics - University of Hasselt, Hasselt, Belgium.

6. Center for Proteomics, University of Antwerp, Antwerp, Belgium.

7. VITO, Mol, Belgium.

8. Institute of Medical Sciences, Banaras Hindu University, Varanasi, India

9. BP Koirala Institute of Health Sciences, Dharan, Nepal

10. Department of Biomedical Sciences, University of Antwerp, Antwerp, Belgium.

* These authors share senior authorship

Corresponding authors

Abstract

Aneuploidy causes system-wide disruptions in the stochiometric balances of transcripts, proteins, and metabolites, often resulting in detrimental effects for the organism. The protozoan parasite *Leishmania* has an unusually high tolerance for aneuploidy, but the molecular and functional consequences for the pathogen remain poorly understood. Here, we addressed this question *in vitro* and present the first integrated analysis of the genome, transcriptome, proteome, and metabolome of highly aneuploid *Leishmania donovani* strains. Our analyses unambiguously establish that aneuploidy in *Leishmania* proportionally impacts the average transcript- and protein abundance levels of affected chromosomes, ultimately correlating with the degree of metabolic differences between strains. This proportionality was present in both proliferative and non-proliferative *in vitro* promastigotes. However, protein complex subunits and non-cytoplasmic proteins, showed dosage compensation, responding less or even not at all to aneuploidy-induced dosage changes. In contrast to other Eukaryotes, we did not observe the widespread regulation at the transcript level that typically modulates some of the negative effects of aneuploidy. Further, the majority of differentially expressed proteins between aneuploid strains were encoded by non-aneuploid chromosomes and were not driven by a significant underlying transcript change, suggesting that aneuploidy is accompanied by extensive post-transcriptional protein-level modulation. This makes *Leishmania* a unique Eukaryotic model for elucidating post-transcriptional protein-abundance modulation in the context of aneuploidy.

Introduction

Aneuploidy is the presence of an abnormal number of chromosomes in a cell. All genes encoded by aneuploid chromosomes undergo a shift in their copy number or "gene dosage". This large number of unbalanced dosage changes typically leads to broad-scale disruptions in the stoichiometric balances of transcripts, proteins, and metabolites, making aneuploidy most widely known for its detrimental effects. Indeed, aneuploidy can cause oxidative stress, energetic stress, misfolded protein stress (proteotoxicity), and metabolic stress at the cellular level [1,2]. In multicellular organisms, where cells are closely fine-tuned to work together, this often leads to growth delays or lethality [1].

Contrastingly, aneuploidy can also result in fitness gains. In fungi, specific karyotypes confer resistance against drugs, toxicants, or increase survival under nutrient limiting conditions [3-6]. Likewise, in cancer cells, aneuploidy can be tumor growth-promoting [7]. By altering the copy number of many genes at once, aneuploidy enables cells to explore a wide fitness landscape [8]. Particularly when facing very novel or competitive conditions, aneuploidy might allow the rapid selection of a beneficial phenotype from a pool of many divergent phenotypes [9]. Fully understanding this complex trade-off between aneuploidy fitness gains and losses requires a systems biological comprehension of its molecular impact.

In this context, a new and unique Eukaryote model is emerging, *Leishmania*. This protozoan parasite (Euglenozoa, Kinetoplastida) that is transmitted by sand flies and infects humans and various vertebrate animals shows a remarkably high tolerance for aneuploidy. A genomic analysis of 204 *in vitro* cultured *Leishmania donovani* strains uncovered up to 22 aneuploid chromosomes (out of 36) within a single strain [10], while *in vivo*, aneuploidy is less pronounced [11]. All 36 chromosomes have the capacity to become aneuploid and lead to viable parasites [12]. Strikingly, clonal populations of the parasite do not have uniform karyotypes but display a mosaic of them[13]. Single-cell sequencing of two clonal promastigote populations of *L. donovani* identified respectively 208 different karyotypes in 1516 sequenced cells (that were generated in approximately 126 generations) and 117 karyotypes in 2378 cells (56 generations). This high degree of genomic instability and mosaicism could explain the parasite's ability to rapidly select more advantageous karyotypes upon encountering novel *in vivo* or *in vitro* environments [11].

Leishmania also features an unusual gene expression system that is markedly different from most other Eukaryotes. Transcription of protein-coding genes cannot be controlled individually as these

72 lack separate RNA polymerase II promoters. Instead, they are transcribed constitutively in long
73 polycistronic units that span 10's to 100's of functionally unrelated genes [14]. The abundance of
74 individual mRNAs and proteins is still regulated, but essentially post-transcriptionally [11,15]. Thus, the
75 most straightforward evolutionary path towards altered gene expression might be altered gene
76 dosage, which could explain the high incidence of aneuploidy in this organism [11]. While aneuploidy in
77 *Leishmania* is known to directly affect the transcription of encoded transcripts, its molecular impact
78 further downstream remains poorly understood [11,16].

79 Here we present the first study that generated and integrated genome, transcriptome, proteome,
80 and metabolome data of highly aneuploid *L. donovani* strains, *in vitro*. This multi-omics analysis
81 unambiguously demonstrates that aneuploidy in *Leishmania* globally and drastically impacts the
82 transcriptome and proteome of affected chromosomes, ultimately correlating with the degree of
83 metabolic differences between strains. This impact is not restricted to a single life stage as we
84 observed it *in vitro* in both the parasite's proliferative and non-proliferative/infectious promastigote
85 life stages. Interestingly, not all proteins responded equally to dosage changes; through dosage
86 compensation, protein complex subunits and non-cytoplasmic proteins responded less or even not at
87 all to aneuploidy. In parallel, aneuploid *Leishmania* strains here studied also feature a surprisingly
88 high number of regulated proteins from non-aneuploid chromosomes, which are likely post-
89 transcriptionally modulated. Through this integrated 4-'omic approach, we provide a systems-wide
90 view of the molecular changes associated with aneuploidy in *Leishmania*.

Methods

Parasites

The experiments in this study were performed on six cloned strains of *Leishmania donovani*: BPK275/0 cl18 (BPK275), BPK173/0 cl3 (BPK173), BPK282 cl4 (BPK282), BPK288/0 cl7 (BPK288), BPK178/0 cl3 (BPK178), BHU575/0 cl2 (BHU575) (**Supplementary Table S1.A**). A strain is a parasite population derived by serial passage *in vitro* from a primary isolate (from patient) with some degree of characterization, in our case bulk genome sequencing (definition modified from [17]). These strains were cloned to ensure genomic homogeneity. Parasites were cultured in HOMEM (Gibco) supplemented with 20% heat-inactivated fetal bovine serum (Biochrom), three days for replicative forms (LOG growth phase, 4-6 replicates) and six days for non-replicative forms (STAT, 4 replicates). Parasites from all replicates were washed twice by centrifugation at 18,000 x g at 0°C, resuspension in ice-cold PBS buffer (PBS; pH 7.4 – Invitrogen), and pelleted at 18,000 x g at 0°C. DNA, RNA, protein, and metabolite extractions were carried out in parallel (see further).

DNA/RNA extraction, library preparation, and sequencing

DNA and RNA were extracted from the parasite pellets with the AllPrep DNA/RNA Mini Kit (Qiagen). The RNA integrity was then verified with the RNA 6000 Nano Kit using a Bioanalyzer 2100 (Agilent). DNA was quantified with the Qubit dsDNA BR assay (Thermo Fisher Scientific) and RNA with the Qubit RNA HS Assay.

Library preparation and sequencing of the DNA samples were performed at the Beijing Genomics Institute (BGI). Libraries were prepared with the TruSeq Nano DNA HT sample prep kit (Illumina) and 2 x 151 bp sequenced on the Illumina HiSeq 4000 platform. RNA sequencing libraries were prepared using the Spliced leader sequencing (SL-Seq) method as described in Cuypers et al. (2017) [15]. This protocol makes use of the presence of the affixed 39 nucleotide sequence spliced-leader (SL) that is present at the 5' end of all functional *Leishmania* mRNAs. RNAs containing a SL are selectively amplified with the protocol, and adapters required for Illumina sequencing are ligated. The SL-Seq libraries were 1 X 50 bp sequenced with the HiSeq 1500 platform of the Center of Medical Genetics Antwerp (Belgium).

Genome and Transcriptome data analysis

The quality of the raw sequencing data was verified with FASTQC v0.11.4 [18]. Reads were quality trimmed using Trimmomatic v035 [19] with the settings 'LEADING:20 TRAILING:20 5

121 ILLUMINACLIP:adapter.fa:2:40:15 SLIDINGWINDOW:4:20 MINLEN:36'. Reads were subsequently
122 aligned to the *L. donovani* LdBPKv2 [20] reference genome using BWA Mem version 0.7.15 [21] with
123 default parameters. The resulting bam files were sorted and indexed with samtools [22]. Mapping
124 reports were generated using samtools flagstat.

125 Somy estimations and gene copy numbers were calculated as described in Downing (2011) [23]. Briefly,
126 the somy value of a chromosome (S) was calculated by dividing its median sequencing depth (i.e. the
127 number of times a nucleotide is read during sequencing, d_{ch}) by the median d_{ch} of all 36
128 chromosomes (d_{mch}) and multiplying this value by two (for a predominantly diploid organism). Gene
129 copy number per haploid genome (d) was defined as a raw depth for that gene (d_r), divided by the
130 median depth of its chromosome (d_{ch}): so that $d = d_r/d_{ch}$. Somy values in our bulk-sequencing
131 analyses are often not discrete due to mosaic aneuploidy (i.e. presence of different kayotypes among
132 individual cells present in 1 strain) in *Leishmania*. Gene copy number estimations per cell (full depth,
133 gene dosage) were then calculated by multiplying d with S. SNPs were previously characterized in [10].
134 RNA-Seq gene read count tables were generated with the HTSeq tool version 0.6.1 [24]. Count data
135 were normalized for library size by dividing each transcript count by the geometric mean of all counts
136 for that library [25].

137 **Proteomics**

138 *Sample preparation*

139 Cell pellets were efficiently lysed using 200 µl RIPA buffer and 1x HALT protease inhibitor (Thermo
140 Scientific), combined with a 30 sec sonication (Branson Sonifier SLPe ultrasonic homogenizer,
141 Labequip, Ontario, Canada) with an amplitude of 50% on ice. After centrifugation of the samples for
142 15 min at 10,000 g at 4 °C, the cell pellet was discarded. Next, the protein concentration was
143 determined using the Pierce BCA protein Assay kit in combination with a NanoDrop 2000
144 photospectrometer (Thermo Scientific).

145 For each sample, 25 µg of proteins were reduced using 2 µl of 200 mM tris(2-carboxyethyl)
146 phosphine, in a volume of 20 µl 200 mM triethylammonium bicarbonate (TEAB), and incubated for 1
147 h at 55℃. After alkylation of the proteins with 2µL of 375 mM iodoacetamide for 30 min protected
148 from light, 6 volumes of ice-cold acetone were added, and the samples were incubated overnight at -
149 20°C. The next day, samples were centrifuged for 10 min at 10.000 g at 4°C, the acetone was
150 removed, and pellets were resolved in 20 µl of 200 mM TEAB. Proteins were then digested with
151 trypsin (Promega) overnight at 37°C with an enzyme trypsin ratio of 1:50. Before LC-MS/MS analysis,

152 the samples were desalted with Pierce C18 spin columns according to the manufacturer's
153 instructions (Thermo Scientific).

154 *Nano reverse-phase liquid chromatography and mass spectrometry*

155 Each of the digested samples was separated by nano reverse phase C18 (RP-C18) chromatography on
156 an Easy-nLC 1000 system (Thermo Scientific, San Jose, CA) using an Acclaim C18 PepMap®100 column
157 (75 µm x 2 cm, 3 µm particle size) connected to an Acclaim PepMap™ RSLC C18 analytical column (50
158 µm x 15 cm, 2 µm particle size) (Thermo Scientific, San Jose, CA). Of each sample, a total of 1µg of
159 peptides were loaded on the column. Before loading, digests were dissolved in mobile phase A,
160 containing 2% acetonitrile and 0.1% formic acid, at a concentration of 1µg/10µL and spiked with 20
161 fmol Glu-1-fibrinopeptide B (Glu-fib, Protea biosciences, Morgantown, WV). A linear gradient of
162 mobile phase B (0.1% formic acid in 100% acetonitrile) from 0 to 45% in 90 min, followed by a steep
163 increase to 100% mobile phase B in 10 min, was used at a flow rate of 300 nL/min. Liquid
164 Chromatography was followed by MS (LC-MS/MS) and was performed on a Q-Exactive Plus mass
165 spectrometer equipped with a nanospray ion source (Thermo Fisher, Waltham, MA, USA). The high-
166 resolution mass spectrometer was set up in an MS/MS mode where a full scan spectrum (350 – 1850
167 m/z, resolution 70,000) was followed by a high energy collision activated dissociation (HCD) tandem
168 mass spectra (100 – 2000 m/z, resolution 17,500). Peptide ions were selected for further
169 interrogation by tandem MS as the twenty most intense peaks of a full scan mass spectrum. The
170 normalized collision energy used was set at 28%. A dynamic exclusion list of 20 sec for the data-
171 dependent acquisition was applied.

172 *Proteomic Data Analysis*

173 Thermo raw files were converted to mzML files using MSConvert v3.0. Label-free protein
174 quantification (LFQ) was carried out with MaxQuant version 1.6.0.16 [26] using the following settings
175 (other settings were kept default): Oxidation (M) and acetyl (Protein N-term) were indicated as
176 variable modifications, carbamidomethyl (C) was indicated as a fixed modification, digestion with
177 trypsin with maximum two missed cleavages, match between runs = yes, dependent peptides = yes.
178 The search database was the LdBPKV2 proteome previously published by our group [11], and reversed
179 proteins were used as decoys.

Metabolomics

Sample preparation

Sample pellets were extracted using a 1:3:1 (v:v:v) chloroform/methanol/water extraction, subjected to liquid chromatography using a 2.1 mm ZIC-HILIC column (Sequant), and analyzed using the Orbitrap Exactive (Thermo Fisher Scientific) platform at the Glasgow Polyomics Center (University of Glasgow, Glasgow, Scotland) exactly as described elsewhere [27,28]. Both negative and positive ion modes were run in parallel with rapid polarity switching. Samples were analyzed in randomized order and the same analytical batch. Additionally, to aid accurate metabolite identification, verify LC-MS stability, and identify contaminants, the following control samples were included as well: (1) solvents blanks, (2) serial dilutions of a pooled sample (Undiluted, 1/2, 1/4, 1/8, and 1/16), (3) Authentic standard mixes containing in total 217 metabolites (50–400 Da) and representing a wide array of metabolic classes and pathways, (4) An amino acid standard mix (Sigma Product No. A9906).

Metabolomic data analysis

Data preprocessing was carried out with the XCMS 1.42.0 [29] and mzMatch 1.0.1 [30] packages in R, exactly as described elsewhere [31]. Briefly, raw spectra (mzXML format) were first subjected to retention time alignment with ObiWarp [32], after which peak detection was carried out with the centWave algorithm [33]. Peaks were then filtered: 1) Corresponding peaks from the four biological replicates were allowed a maximum reproducibility standard deviation (RSD) of 0.5, 2) Peak shape (CoDA-DW > 0.8), 3) Detection in at least 3 out of 4 replicates of a single strain and 4) Minimal peak intensity was set to 3000. The peaks were putatively identified using sequentially the LeishCyc database [34], LIPID MAPS [35], KEGG [36], the peptide database included in mzMatch, and the Human Metabolome Database [37]. Finally, the filtered peaks were normalized for total ion count and subjected to manual quality screening.

Integrated multi -omic analysis

Pairwise comparisons between aneuploid strains: For each comparison between two strains, we calculated the Log_2 fold change (Log_2FC) for genes (gene dosage), transcripts, proteins and metabolites. These Log_2FC values were obtained by taking the Log_2 ratio of the average abundance between two strains. Associated *p*-values were obtained by performing a Student *t*-test for each comparison and subsequently correcting it with the Benjamini-Hochberg algorithm to limit the False Discovery Rate (FDR) to 5%. A Log2FC cutoff of 1 and adjusted *p*-value cutoff of 0.05 was used for all

210 'omic layers, except for gene dosage, for which only copy number differences of at least 0.5/haploid
211 genome were considered as biologically significant [38].

212 Average transcript and protein abundance levels per chromosome per strain (Fig 1 C): First, the
213 median was taken of the Log_2 normalized transcript counts (see respective section) and Log_2 LFQ
214 protein values, per chromosome per strain. This yielded an expression value for each chromosome in
215 each strain, for both transcript and protein expression. Then, for each chromosome, the expression
216 value of the strain that was the most disomic (determined based on DNA sequencing data) for that
217 chromosome was selected and was further used as the 'disomic reference value' for that
218 chromosome (i.e., the expression value that corresponds to the median expression of a
219 transcript/protein on a disomic chromosome). The remaining per-strain per-chromosome expression
220 were then divided by this disomic reference value, multiplied by 2, and plotted in Figure 1C. The code
221 for these normalizations and analyses is available at
222 (https://github.com/CuypersBart/Leishmania_Multiomics).

223 All plots were generated using the ggplot v 2_2.1.0 package [39], except the Circos plots which were
224 created with Circos v0.69 [40]. Gene ontology enrichments were calculated with the Fisher Exact test
225 using Python 3.8.5 and the matplotlib v3.3.4 [41] and SciPy v1.6.1 [42] libraries. GO annotations were
226 obtained from the gene ontology consortium (http://www.geneontology.org/).

227 Dosage compensation analysis

228 Dosage compensation analysis (Figure 2): This analysis was carried out on the only three
229 chromosomes (Ld05, Ld08, and Ld33) that were at least once disomic (somy of 1.7-2.3), trisomic
230 (somy of 2.7-3.3), and tetrasomic (somy of 3.5 or more) in our six study strains and had more than 10
231 detected proteins. The abundance values of transcripts (corrected for library size, see above) and
232 proteins (LFQ) were divided by their abundance in the strain that was the most disomic for their
233 encoding chromosome, according to the genome sequencing data. These expression values were
234 then multiplied by 2 so that the normalized abundance at disomy = 2. Strains were always
235 normalized by another strain than themselves to avoid underestimation of the standard deviation.
236 Therefore, we do not have disomic distributions for Ld08 since Ld08 was exclusively disomic in
237 BPK282, and thus already was used as reference strain.

238 Functional dosage compensation analysis: For this analysis, we defined a protein's compensation
239 level as its Log_2 transcript fold change (i.e., its transcript level on the aneuploid chromosome divided
240 by its transcript level on disomic chromosome), minus its Log_2 protein fold change. We included only

241 85 transcripts and proteins for this analysis, which had very accurate protein measurements (SD
242 between biological replicates < 0.25 Log_2FC units). The following protein features were checked for
243 their relation with protein dosage compensation: degree (i.e., number of protein interactions as
244 transferred from STRING), length (as a proxy for transcript and protein molecular size), GRAVY (grand
245 average of hydropathy), solubility (soluble versus membrane protein) and subcellular location. We
246 added transcript abundance as a covariate to the model, as the compensatory effect can be expected
247 to become larger at higher differential transcript levels. The code these normalizations and analyses
248 is available at (https://github.com/CuypersBart/Leishmania_Multiomics).

Results

Aneuploidy globally impacts transcriptome and proteome of affected chromosomes

We examined the impact of aneuploidy in *L. donovani* on transcriptome and proteome by integrated multi-omic analysis of 6 *L. donovani* strains from India and Nepal (**Suppl. Table S1.A**). These closely related strains are almost identical at the sequence level but differ greatly in their aneuploidy [43]. Specifically, the entire genome between any two strains of this set differs at most by 64 non-synonymous SNPs and one indel in coding regions (**Suppl. Table. S1.B)**. Thus, they are attractive model strains for studying the impact of aneuploidy on transcriptome and proteome with minimal interference of DNA sequence variation.

Genome, transcriptome, and proteome were obtained from the *in vitro* replicative promastigote stage (LOG) of the parasite. All genomes reached an average sequencing coverage of at least 26.5 fold, and 97.9 % of the sequenced sites reached 10 X coverage or more. Transcript samples had on average 4.71 million reads and obtained an average mapping efficiency of 97%. Detailed mapping and coverage statistics for both genome and transcriptome data are available in **Suppl. Table S1.C/S1.D.** Identified indels and estimations of chromosomal somy (i.e., average chromosome copy number in the population of cells) and dosage of each gene in **Suppl. Table S2**. Identified transcripts and their counts are available in **Suppl. Table S3**. Proteome analysis identified in total 3145 proteins across all samples (**Suppl. Table S4**).

Our 6 *L. donovani* strains showed high but varying degrees of aneuploidy (**Fig 1A**). The most aneuploid strain was BPK288 with 12 aneuploid chromosomes, followed by BPK275 (10), BPK173 (10), BHU575 (10), BPK178 (9), and BPK282 (6). In *L. donovani,* chromosomes are numbered by increasing size. The baseline somy of chromosomes in *L. donovani* is 2N, except for chromosome 31, which is always 4N or more. Smaller chromosomes were more frequently aneuploid (Ld01, Ld05-Ld09, Ld11-Ld16), than larger chromosomes (Ld20, Ld23, Ld26, Ld31, Ld33, Ld35). Chromosome Ld31 was confirmed tetrasomic in all strains, and chromosome Ld23 always trisomic. Other aneuploid chromosomes had a variable somy. In bulk genomic analysis, somy values represent the average of the somy of individual cells present in a given population. Because of mosaicism, i.e. the presence of different karyotypes among individual cells of the parasite population in culture, many somy values were not discrete. The highest somy values (apart from Ld31) were observed for chromosomes Ld02 (somy = 3.9), Ld08 (3.9), and Ld33 (3.5) in BPK275, and for chromosome Ld05 (3.6) in BPK288.

279 The transcript abundance of aneuploid chromosomes mirrored almost perfectly their underlying
280 somy (**Fig 1B, Suppl. Fig S1A, S1B**). Specifically, the average abundance of a transcript encoded by a
281 chromosome was proportional with a factor of 0.94 with the chromosomal somy (**Fig 1C**: 95% CI:
282 0.92 – 0.96 and $p < 2 \cdot 10^{-16}$, R^2: 0.98). The average abundance of the proteins encoded by a
283 chromosome was also highly proportional to the aneuploidy of the chromosome ($p < 2 \cdot 10^{-16}$), albeit
284 with a decreased slope of 0.76 (95% CI: 0.70 - 0.77, R^2: 0.92). Thus, aneuploidy results in a linear, but
285 not equivalent, increase in protein abundance. Circos plots clearly showed that transcript- and
286 protein abundance of aneuploid chromosomes was affected globally and not restricted to specific
287 chromosomal regions (**Fig 1B, Suppl. Fig S1A, S1B**).

288 Interestingly, chromosome 35 exhibited only a partial amplification in strain BPK275, the first part
289 being disomic (somy = 2.2) and the second part, starting from gene LdBPK_350040900, being
290 trisomic (somy = 3.1) **(Fig 1B).** This phenomenon of partial chromosomal amplification has previously
291 been observed for chromosome 23 as well [44,45]. The difference in both average transcript and protein
292 abundance between the first and the second chromosome part was significant (t-test p Trans =
293 4.0×10^{-82}, Prot = 7.0×10^{-7}), the second part having on average 1.43x more transcript abundance and
294 1.22x more protein abundance. This demonstrates that also partial chromosomal amplifications
295 affect transcript and protein abundance proportionally in the amplified region.

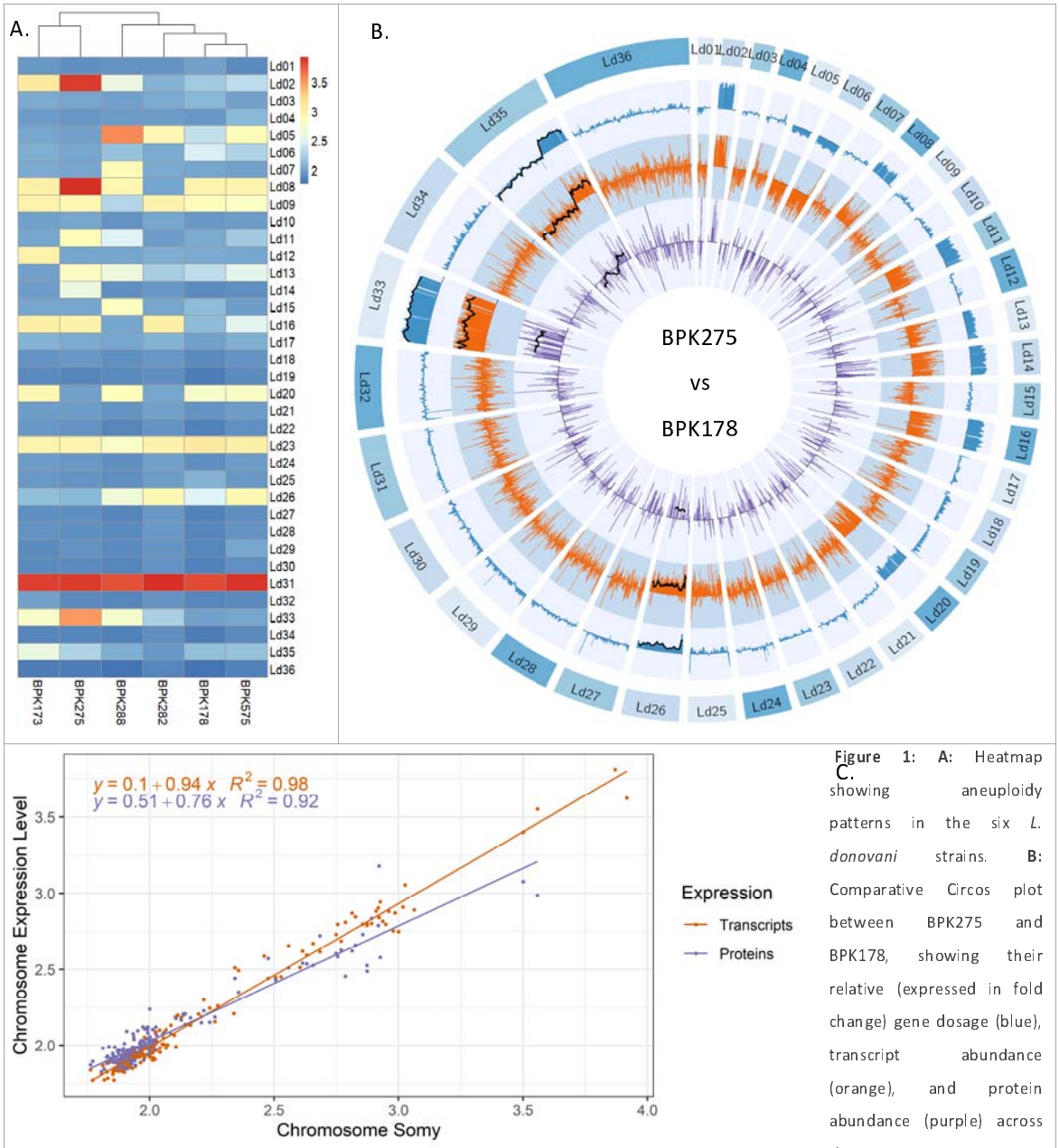

Figure 1: A: Heatmap showing aneuploidy patterns in the six *L. donovani* strains. **B:** Comparative Circos plot between BPK275 and BPK178, showing their relative (expressed in fold change) gene dosage (blue), transcript abundance (orange), and protein abundance (purple) across the 36 *L. donovani* chromosomes. 20 point moving averages are indicated with a black line for the three largest aneuploid chromosomes. We show this strain pair because of the partial chromosomal amplification on chromosome Ld35. However, Circos plots between BPK173 and BPK282, and BHU575 and BPK288 show similar agreement between genome, transcriptome, and proteome and can be found in supplementary figures (Suppl. Fig S1A, S1B). **C**: Impact of chromosome aneuploidy on average chromosome transcript (red) and protein (blue) abundance levels. Each dot represents 1 chromosome in one of the six studied aneuploid *L. donovani* strains in the replicative (LOG) phase. Abundance levels were normalized so that two transcript/protein abundance units match the abundance level of a disomic chromosome. Somy values are often not discrete due to mosaic aneuploidy (i.e. presence of different kayotypes among individual cells present in 1 strain) in *Leishmania*.

296 **Aneuploidy does not impact all proteins equally: dosage compensation in**
297 ***Leishmania***

298 Our observation that a somy increase does not lead to an equivalent increase in protein abundance,
299 but 0.76x the somy change, suggested either of two possible explanations. A first possibility is that all
300 proteins encoded by an aneuploid chromosome are modulated equally and exhibit only a partial
301 protein abundance increase. We further refer to this explanation as the 'dampening hypothesis'.
302 Such a general 'dampening' effect would suggest an underlying process related to intrinsic
303 mechanisms or limitations in the parasite's translation system. Alternatively, different proteins could
304 respond differently to increased gene dosage and transcript abundance, pointing to compensatory
305 effects linked to the identity, function, and physicochemical properties of those specific proteins or
306 certain functional protein groups. We refer to this explanation as the 'compensation hypothesis'.

307 To evaluate both hypotheses, the differential abundance patterns of proteins were compared to
308 their encoding chromosome differences from disomy to trisomy and tetrasomy. Following the
309 'dampening hypothesis', the average of the protein abundance distribution should increase with
310 increased somy, but the distribution shape should remain unaltered. In our study, three
311 chromosomes (Ld05, Ld08, and Ld33) were at least once disomic, trisomic, and tetrasomic in one of
312 our six study strains (**Fig 1B**), allowing for such comparative analysis. Ld02 also matched these criteria
313 but was excluded from the analysis as only nine Ld02 proteins were detected. For reference, the
314 same analysis was conducted for transcripts.

315 The average abundance of transcripts increased with somy, and the shape of the abundance
316 distribution was found to be similar (**Fig 2A**). Specifically, the transcript abundance standard
317 deviation did not significantly change with somy (Regression *p*: 0.10, **Fig 2B**), and the distributions
318 were symmetric. This suggests that a somy change affects most transcripts equally, and dosage
319 compensation at the transcript level is minimal or absent. Chromosome Ld08 had a higher variance in
320 transcript abundance than the two other chromosomes. Our data is not conclusive as to whether this
321 is due to the shift in somy or due to an intrinsically higher transcript abundance variance for this
322 chromosome.

323 The average abundance of proteins also increased with somy, but the distribution shape was not
324 consistent. This was particularly evident when comparing the disomic versus the tetrasomic
325 chromosomes. We observed a clear left-tailing of the protein abundance distribution on
326 chromosomes Ld08 and Ld33 chromosomes towards the lower, more conservative fold change

values. Thus, while a subset of proteins follows the aneuploidy-induced gene dosage changes, another subset is maintained at conservatively lower levels. This dosage compensation was also reflected in a general and significant increase in protein abundance variance for all three chromosomes (Regression *p*: 0.004).

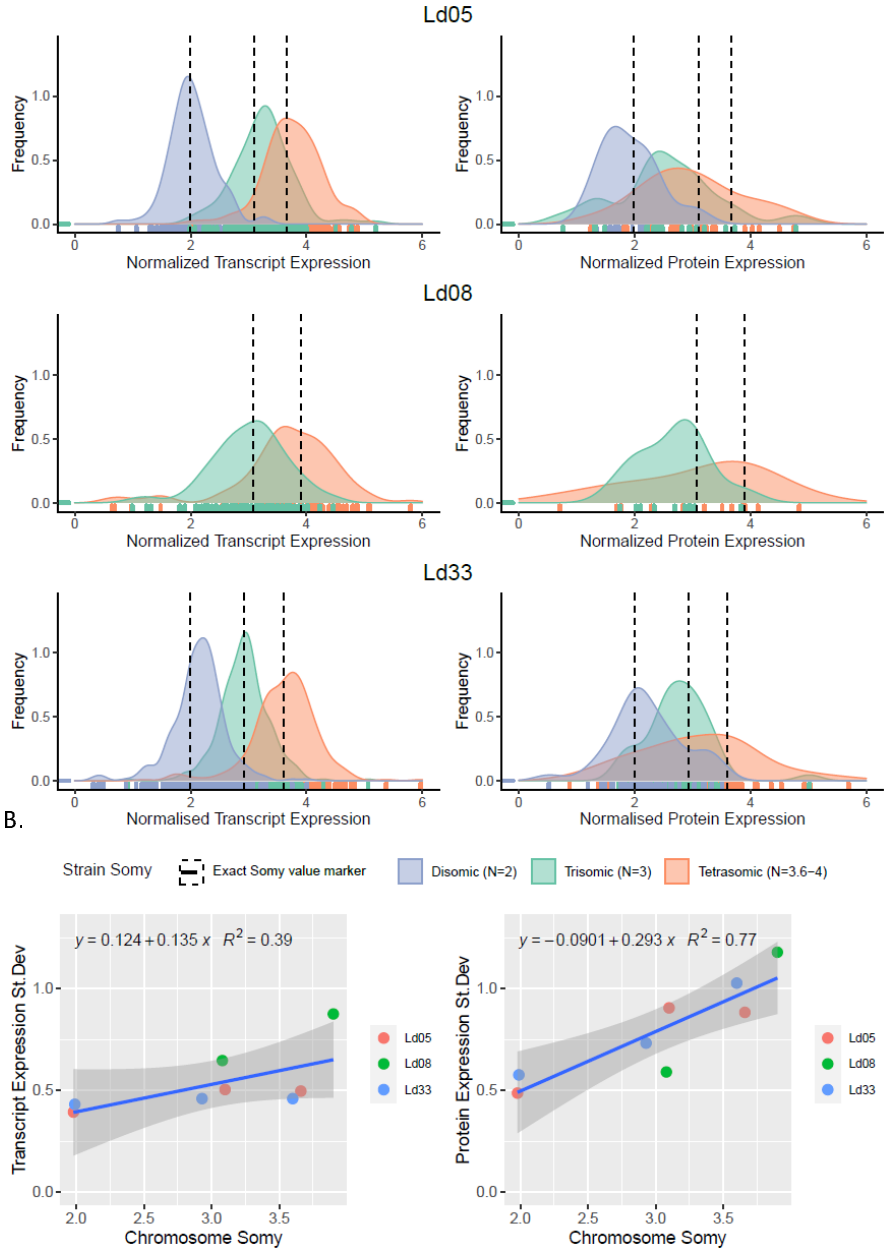

Figure 2: **A**: Normalized transcript (left) and protein (right) abundance distributions of chromosomes Ld05, Ld08, and Ld33 in their disomic (excl. chr 8), trisomic and tetrasomic states, each time observed in one of our 6 study strains. Vertical dotted lines indicate the corresponding somy, derived from the genomic data. The small vertical lines at the base of the plot indicate individual datapoints for transcripts and proteins, from which the distributions were generated. The abundance values of transcripts and proteins were normalized

336 so that the normalized abundance at disomy = 2. This normalization was carried out with a strain that was disomic for the chromosome
337 under investigation. We do not have disomic distributions for Ld08 since Ld08 was exclusively disomic in BPK282, and thus already was
338 used as reference strain. **B.** Regression between the somy and transcript (left) or protein (right) standard deviation for chromosomes Ld05,
339 Ld08, and Ld33 in different somy states.

340 Compensated proteins are primarily protein complex subunits or non-cytoplasmic

341 We investigated if specific protein properties were associated with the dosage compensation
342 observed in our dataset. For this analysis, we defined a protein's compensation level as its Log_2
343 transcript fold change (i.e., its transcript level on the aneuploid chromosome divided by its transcript
344 level on disomic chromosome), minus its Log_2 protein fold change. A particular challenge in this
345 analysis was that protein fold changes, and hence, the observed compensation levels, were generally
346 very small and close to measurement noise levels. For example, for a fully compensated protein from
347 a trisomic chromosome, the compensation level would only be 0.5 Log_2FC units (Log_2FC transcript ≈
348 0.5, Log_2FC protein = 0). Therefore, we focused on a set of 85 transcripts and proteins, which had
349 very accurate protein measurements (SD between biological replicates < 0.25 Log_2FC units). These
350 covered a broad range of compensation levels ranging from 1.18 Log_2FC units, to values close to zero,
351 or even some proteins that had a slight overamplification compared to the transcript level (-0.40
352 Log_2FC units) (**Suppl. Table S1.E**).

353 We noted that within the top 5 most compensated proteins in this high-accuracy set, 2 coded for
354 subunits of protein complexes: e.g., the cleavage and Polyadenylation Specificity Factor (CPSF)
355 subunit A and the dynein light chain had respectively 1.12 and 0.96 Log2FC units lower protein than
356 transcript abundance. Accordingly, we hypothesized that protein complexes might be more likely to
357 be dosage compensated (>= 0.30 Log2FC units). To test this systematically, all 85 proteins were
358 screened for their involvement in heteromeric protein complexes (using annotation keywords
359 'subunit' and 'chain', **Suppl. Table S1.E**). Strikingly, complex subunits accounted for 15.6 % (5 out of
360 32) of the compensated, proteins which was significantly more than the 1.8% (1 out of 53) we
361 observed for the uncompensated proteins (Fischer exact p = 0.0265).

362 Next, we looked if there was a relation between dosage compensation and a set of biological and
363 physicochemical protein properties to identify more subtle patterns. Specifically, we checked 5
364 protein properties for their relationship with protein dosage compensation using AN(C)OVA **(Suppl.
365 Table S1.E)**. Transcript abundance was added as a covariate to the model, as dosage compensation
366 was larger at higher differential transcript levels (Adj $p = 2.4 \times 10^{-4}$). The variables 'membrane protein'
367 (yes or no) (FDR adjusted p = 0.696), the number of protein interactions (Adj. p = 1), protein length (a

368 proxy for transcript and protein size) (Adj. p = 1) and hydrophobicity (Adj. p = 1) had no significant
369 relationship with dosage compensation. In contrast, the subcellular location (Adj. p = 0.032) of a
370 protein was significantly linked to its degree of dosage compensation. To investigate this further, we
371 investigated the relation between each subcellular compartment and the compensation rate of its
372 proteins **(Suppl. Table S1.E)**. Cytoplasmatic proteins (n = 39) were significantly less compensated
373 compared to all other proteins (Adj. p = 0.011). Thus, cytoplasmatic proteins follow aneuploidy-
374 induced dosage changes more closely than proteins from other cellular compartments. In contrast,
375 proteins associated with the Golgi apparatus (n = 2) had a significantly higher compensation than all
376 other proteins (Adj. p = 0.0065). However, this result needs to be interpreted with caution as the
377 sample size was only 2 proteins. These two proteins were a vesicle-associated membrane protein
378 and a small GTP-binding protein Rab18, both known to be secreted. Proteins from mitochondria (Adj.
379 p = 0.32, n = 18), nucleus (Adj. p = 0.50, n = 13), peroxisome (Adj. p = 0.81, n = 6) and ER (Adj. p =
380 0.74, n = 2) did not have significantly different compensation rates compared to proteins from all
381 other compartments.

382 The impact of aneuploid chromosomes on the gene products of their euploid 383 counterparts

384 In the previous sections, we reported how the aneuploidy of a chromosome affects the abundance of
385 its encoded transcripts and proteins. However, through perturbation of regulatory networks, these
386 changes might also affect transcripts and proteins encoded by genomic regions unaffected by
387 aneuploidy. These were previously defined as 'trans-effects' and have been observed on the
388 transcriptional level in diverse species, including humans, yeast, maize, and *Arabidopsis* [46-49]. Here we
389 investigated the extent of trans-effects in *Leishmania* by comparing and characterizing the fractions
390 of differential transcripts and proteins coming from aneuploid chromosomes, i.e. primary or cis-
391 transcripts and cis-proteins [49], versus those coming from euploid chromosomes, i.e. trans-transcripts
392 and trans-proteins.

393 We carried out differential transcript and protein abundance analyses (FDR adjusted $p < 0.05$)
394 between all possible pairs of the six *L. donovani* study strains (**Table 1**). On average, 71.8 % of
395 differentially expressed transcripts were cis-transcripts, while cis-proteins constituted only 40.7 %.
396 The remaining 28.2 % of differentially expressed transcripts and 59.3 % of proteins were thus
397 encoded by euploid chromosomes (trans-) and have therefore been regulated by another mechanism
398 than gene dosage. Interestingly, only 20.0 % of these trans-proteins had a corresponding transcript

399 change (|Log2FC| > 0.5), indicating the vast majority is regulated at protein level directly and not
400 through modulation of mRNA levels. Importantly, none of these trans-transcripts nor trans-proteins
401 were associated with local copy number variants: these were rare and excluded from this analysis.
402 Also sequence variation between strain pairs is unlikely to have resulted in the observed proportions
403 of differential trans-transcripts and trans-proteins. Only 11 trans-transcripts contained SNPs between
404 our strains (6 missense, 1 synonymous and 4 upstream SNPs) and 2 proteins (1 upstream and 1
405 downstream SNP) (Supplementary Tables 1G & 1H). Therefore, our hypothesis is that aneuploidy
406 induces direct changes to cis-transcripts and cis-proteins, which in their turn directly (e.g., protein-
407 protein interaction) or indirectly drive abundance changes in trans-transcripts and mostly, trans-
408 proteins.

409 Next, we looked deeper into the functions of trans-transcripts and proteins. After pooling the trans-
410 transcripts and trans-proteins from all comparisons, we identified a set of 541 unique trans-
411 transcripts and 203 unique trans-proteins (duplicates and hypothetical proteins removed, **Suppl.**
412 **Tables S1.G & S1.H**). GO-overrepresentation analysis showed that no GO terms were significantly
413 enriched in the pooled list of trans-transcripts or trans-proteins from all comparisons (FDR adjusted *p*
414 threshold 0.05). However, it must be noted here that GO- and other annotations in *Leishmania* are
415 often relatively unspecific due to the parasite's distinct evolutionary position, and therefore low gene
416 homology with better studied model organisms. For example, only 48.7% of the *L. donovani* genes
417 could be annotated with at least one GO term, and even these are often of the highest hierarchies
418 (low specificity)[11]. As an alternative enrichment analysis approach using the full genomic annotations
419 directly, we first manually checked if any frequent keywords could be observed occurring in
420 annotations of the trans-proteins and identified 10. We then compared if these keywords were
421 significantly enriched versus all detected proteins with a Fisher Exact test. 7 of these were indeed
422 significantly enriched of which 3 related to protein metabolism: peptidase activity (Adj. $p = 9.4 \times 10^{-}$
423 ^{5}), heat-shock protein (Adj. $p = 2.3 \times 10^{-2}$) and chaperon(in) (Adj. $p = 2.1 \times 10^{-2}$), 2 related to
424 metabolism: glutamate (Adj. $p = 1.9 \times 10^{-2}$) and long-chain-fatty-acid-CoA ligase (Adj. $p = 5.4 \times 10^{-3}$),
425 and two others: mitochondrial (Adj. $p = 3.0 \times 10^{-2}$) and hypothetical protein (FDR adjusted $p = 3.4 \times$
426 10^{-7}). At RNA-level none of the keywords were significant. This demonstrates that differential trans-
427 proteins associated with aneuploidy are not a random occurrences, but related to specific functional
428 classes and processes. Particularly relevant in this context are the enrichment of heat-shock proteins
429 and chaperones, as aneuploidy is known to burden protein folding pathways[50].

430 **Table 1:** Total numbers (N) of differential (FDR adjusted $p < 0.05$) transcripts and proteins between all possible pairs of our 6 *L.donovani*
431 strains. Each time, it is indicated what proportion of these transcripts or proteins originate from chromosomes that have somy changes
432 (because of aneuploidy) in the strain pair (Cis) or chromosomes that have identical somies between the two strains (Trans). Five
433 comparisons are not shown because they contained less than 15 differential transcripts or proteins. These are shown in Supplementary
434 table 1F.

	DIFFERENTIAL TRANSCRIPTS			DIFFERENTIAL PROTEINS		
STRAIN COMPARISON	Cis (%)	Trans (%)	N	Cis (%)	Trans (%)	N
275vs178	79.8	20.2	386	44.8	55.2	105
275vs173	86.6	13.4	134	40.7	59.3	91
275vs282	77.6	22.4	67	46.4	53.6	84
288vs282	60.9	39.1	23	39.3	60.7	61
275vs575	84.8	15.2	145	58.9	41.1	56
173vs288	86.3	13.8	80	55.6	44.4	27
173vs282	74.4	25.6	39	48.1	51.9	27
173vs178	55.0	45.0	40	26.3	73.7	19
575vs282	41.2	58.8	34	6.3	93.8	16
AVERAGE	71.8	28.2		40.7	59.3	

435

436 ## Aneuploidy globally affects transcriptome and proteome regardless of life stage

437 So far, this study discussed results from the logarithmic growth stage (LOG), which essentially
438 consists of *Leishmania* procyclic promastigotes (replicating, non-infectious). However, despite the
439 absence of transcriptional regulation of individual protein-coding genes, transcripts and proteins can
440 undergo post-transcriptional regulation during parasite differentiation. This raised the question
441 whether the correlation between chromosome somy, average transcript abundance, and average
442 protein abundance is also present in other life stages. Hence, for three strains, we compared the LOG
443 growth with the STAT growth phase. STAT is highly enriched for metacyclic promastigotes, which are
444 non-replicating, have a distinct morphology, are metabolically different, and infectious to the human
445 host [51]. This was validated with metacyclogenesis markers META1 and HASPB, which were
446 significantly upregulated in STAT as they are expected to be (Adj. $p < 10^{-13}$, **Suppl. Table 1.H**).
447 Transcriptome and proteome measurements and analyses were carried out exactly as for the LOG
448 phase.

449 For both LOG and STAT, a chromosome's somy was proportional to its average transcript expression
450 level, and protein expression level (**Fig 3**, $p < 2 * 10^{-16}$ for transcript and protein in both LOG and
451 STAT). Dosage compensation was apparent at the protein level, in both LOG and STAT growth

452 phases. This suggests that the gene dosage effects associated with aneuploidy remain present
453 throughout the parasite's life cycle.

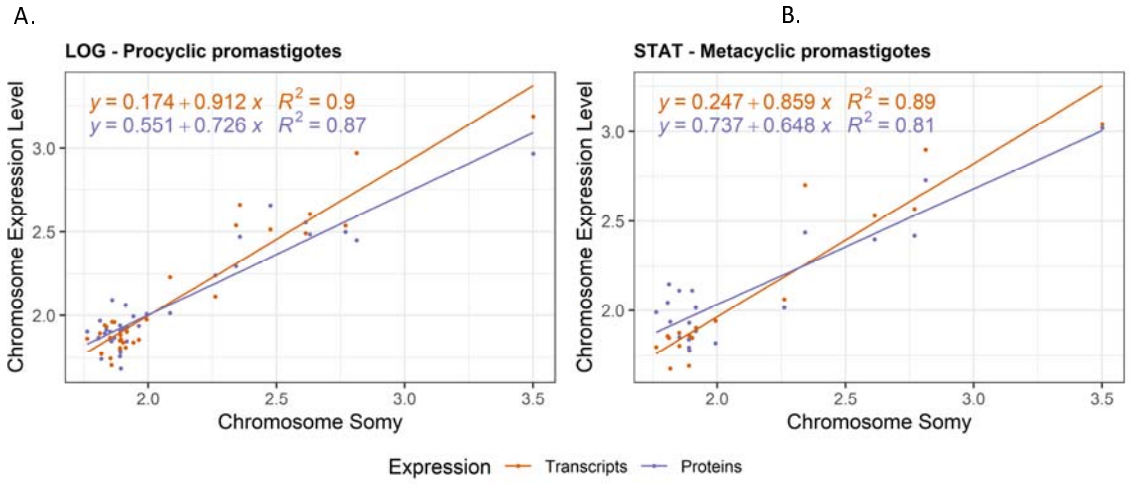

454

455 **Figure 3:** Impact of chromosome aneuploidy on average chromosome transcript (red) and protein (blue) output levels in
456 LOG phase (A) and STAT phase (B). Each dot represents 1 chromosome in one of the 3 studied aneuploid *L. donovani* strains
457 (BPK275, BPK178, and BPK173).

458 Aneuploidy results in metabolic differences between *L. donovani* strains

459 We ultimately aimed to understand if aneuploidy in *L. donovani* is reflected in the parasite's
460 metabolome. Therefore, we carried out LC-MS metabolomics and confidently identified 78
461 metabolites across the six aneuploid study strains (**Suppl. Table S5**). In contrast to transcripts and
462 proteins, there is no straightforward relation between a metabolite and a specific gene. Genes might
463 affect metabolites directly (e.g. an enzyme), indirectly, affect multiple metabolites, or affect no
464 metabolite at all. Therefore, we turned to an indirect strategy to integrate the metabolomic data
465 with our previous observations.

466 We determined if differences in aneuploidy between strains in LOG correlate with their metabolic
467 differences. As such, we calculated the pairwise genomic (somy), transcriptomic, proteomic, and
468 metabolic Euclidean distance (based on all measured chromosomes, transcripts, proteins and
469 metabolites) between each possible strain pair, and correlated these distances (**Fig 4**). The larger the
470 distance between these 2 strains, the more different their respective genomes, transcriptomes,
471 proteomes, or metabolomes are from one another. Consistent with our other analyses, we found
472 strong correlations between the genomic and transcriptomic distance, between the transcriptomic

473 and proteomic distance, and between the genomic and proteomic distance ($p \leq 0.001$ for all
474 comparisons). However, the metabolome initially did not show any correlation with genome,
475 transcriptome, and proteome. We suspected this might be caused by the high intrinsic levels of
476 random variation of a subset of metabolites (by either technical or biological causes). Therefore, in
477 the second phase of the analysis, we filtered on metabolites that had at least once a significant fold
478 change (adjusted $p < 0.05$) between any pair of two strains. This strategy selects only metabolites
479 that are stable enough to reflect true differences in metabolite levels between strains. The resulting
480 'differentiating metabolome' consisting of 34 metabolites correlated strongly with all omic layers ($p <$
481 0.05, Fig 4). This demonstrates that the degree of karyotype difference between two strains
482 correlates with their degree of metabolic differences. Specifically, the differentiating metabolome
483 included 9 amino acids (alanine, aspartate, cysteine, leucine/isoleucine (not distinguishable),
484 methionine, phenylalanine, tryptophan, tyrosine, and valine), suggesting the amino acid metabolism
485 is an important molecular difference between these aneuploid parasites.

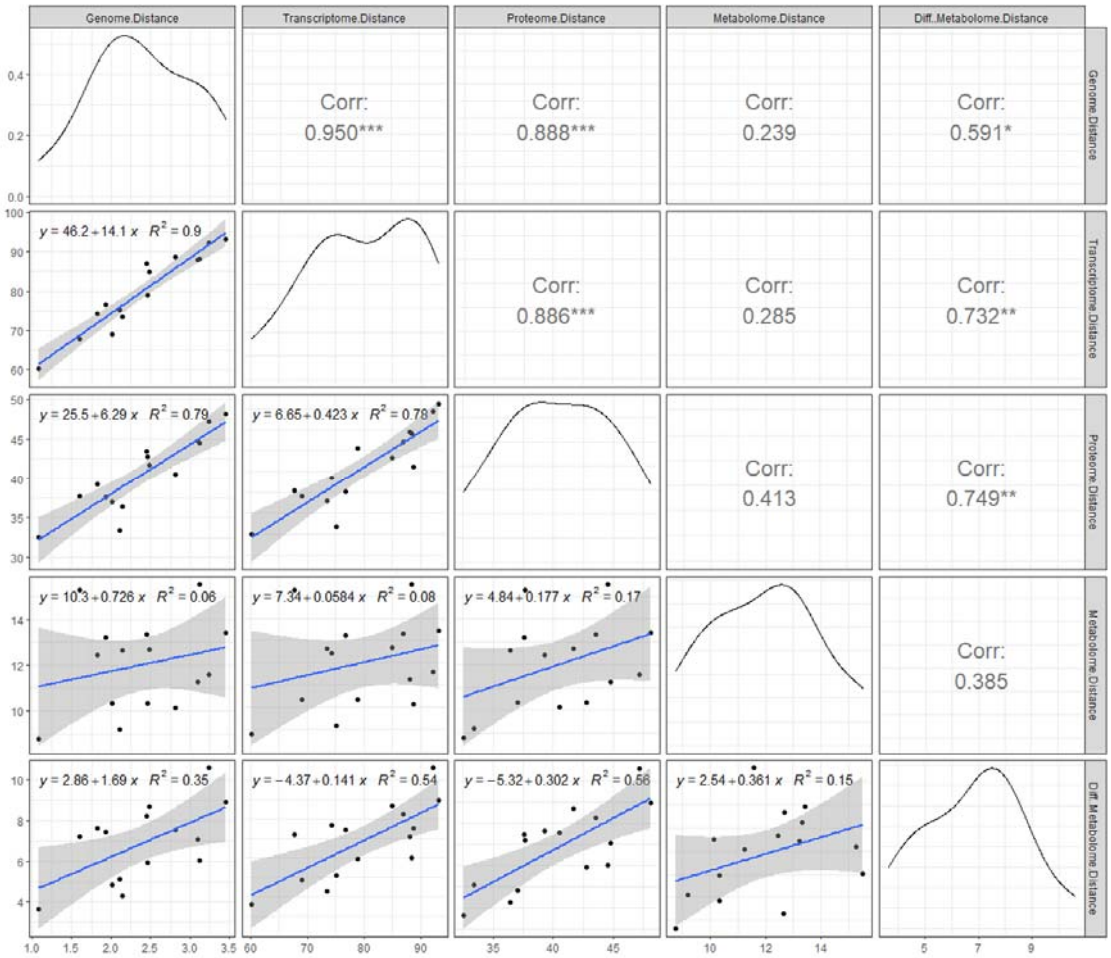

Figure 4: How differences between two *L. donovani* strains on 1 'omic layer correlate with their differences on another omic layer. The plots show the pairwise correlations between the genome distance (aneuploidy), transcriptome distance, proteome distance, metabolome distance (all 78 metabolites), and differentiating metabolome distance (34 metabolites), each time calculated between 2 *L. donovani* strains. Each dot represents 1 comparison between two strains. With 6 strains in our experiment, there were 15 possible pairwise comparisons. The distance metric that was used is the Euclidean distance. Somy values were used directly, but transcript abundance, protein abundance or metabolite abundance were first Z-scored before calculating the distance. The top-right panels show the Pearson correlation coefficients with * = Pval <0.05, ** Pval <0.01, *** = Pval <0.001, while the bottom-left panels show the linear regressions.

Discussion

Leishmania displays a remarkably high tolerance for aneuploidy, with any chromosome having the capacity to become polysomic and produce a viable parasite. The high karyotype dynamicity and the drastic karyotype changes between experimental conditions stress the central importance of aneuploidy for the parasite to adapt to novel environments [10]. However, it remained unclear how this large genomic unstability affects the parasite as a system. Moreover, *Leishmania*'s distinct phylogenetic status and unique gene expression system disallows extrapolation from model systems. Therefore, we investigated the systemic impact of aneuploidy in *L. donovani* by integrating, for the first time, genome, transcriptome, proteome, and metabolome profiling data of highly aneuploid strains. Our study offers a comprehensive picture of the molecular changes associated with aneuploidy in this unique Eukaryotic model that lacks transcriptional regulation of individual protein-coding genes.

We confirmed that transcript abundance is affected across the entirety of aneuploid chromosomes. This observation is in line with previous work that has also found a strong link between aneuploidy-induced gene dosage changes and transcript abundance in *Leishmania* [11,16,52]. We further showed that this relation is almost equivalent, with transcription levels closely mirroring chromosome copy number changes (transcript abundance = 0.94x the somy). It is important to note here that to establish this 0.94x equivalence, we compared the same chromosome to its own disomic state as the reference transcript expression level at disomy. This does not exclude that chromosomes (or, on a smaller scale, cistrons) can have inherently different transcription levels. Indeed, it has previously been shown that chromosome 31 has the expression of a disomic chromosome in its default tetratomic state[16]. The impact of aneuploidy on the *L. donovani* proteome was also linear and chromosome-wide, but not equivalent. For every chromosome copy, the protein abundance levels of that chromosome increased (on average) by a factor 0.76x the somy.

This reduced impact of gene dosage on the protein level was due to the compensation of a subset of proteins. While many proteins did follow the aneuploidy-induced gene dosage changes, the dosage of a subset was compensated. This compensation ranged from partial to complete compensation to disomic levels. Our data thus suggest that the abundance of these proteins is somehow post-transcriptionally attenuated in response to a dosage change. We made two observations concerning the identity of compensated proteins that might explain this attenuation. Firstly, compensated proteins were enriched for subunits of macromolecular protein complexes (15.6% versus 1.8% in the

527 background set). This observation matches several observations in aneuploid yeast and human
528 (including cancer) cell lines [46,47,53-56] that also detected protein complex subunits to be highly
529 prevalent amongst compensated proteins. It can be explained by the fact that individual subunits of
530 macromolecular complexes are typically unstable unless assembled into a stable complex [46]. As
531 subunits of a single complex are often encoded on different chromosomes and produced in balanced,
532 stoichiometric amounts, an increase in an individual subunit (here: by aneuploidy) will often not lead
533 to more complex formation [46,47,57]. Instead, the protein will not have an available binding partner(s),
534 remains unstable, and rapidly degrades. Possibly, this stochiometric imbalance caused by aneuploidy
535 is somehow detrimental to the parasite. One argument in this direction is that we and previous
536 studies found smaller *Leishmania* chromosomes to be more frequently aneuploid, which matches
537 observation in yeast and humans (chromosome 21 has the smallest number of genes in humans and
538 the least severe autosomal aneuploid) [10,23,58]. Additionally, it has been shown in yeast that genes that
539 are deleterious when overexpressed are enriched for protein complex subunits[59]. Secondly, we
540 observed a correlation between the degree of compensation and the cellular destination of the
541 compensated protein. Two secreted proteins associated with the Golgi apparatus were the most
542 compensated (i.e. their expression was close to disomic levels), which could be explained by the fact
543 that secreted proteins do not accumulate in the cell. Correspondingly, dosage compensation of
544 secreted proteins was also observed in a recent study of human fibroblasts with trisomy 21 [46].
545 Proteins from mitochondria, the nucleus, and the peroxisome were also significantly more
546 compensated than cytoplasmatic proteins, which had the lowest level of compensation (i.e.,
547 cytoplasmic proteins followed gene dosage the best). A potential explanation might be that
548 mitochondrial, nucleic, and peroxisome proteins require active transport into their destined
549 organelle. This transport requires extensive interaction with other proteins, potentially explaining
550 why their abundance scales less with increased protein production. In aneuploid (disomic II) strains
551 of *S. cerevisiae*, increased translation was found of genes related to protein trafficking pathways of
552 the endomembrane system and nucleus, also suggesting dependency on this system [60].

553 Partial chromosomal amplification can occur in *Leishmania*. We have previously observed this
554 phenomenon for chromosome Ld23 [44,45] and in the present study for Ld35. Interestingly, gene dosage
555 proportionally affected transcript and protein abundance for these subchromosomal amplification as
556 well. This suggests that our findings can be extrapolated to segmental aneuploidy as well.

557 Further, we demonstrated that these gene dosage changes remain important throughout at least
558 several life stages of the parasite. Indeed, we observed an similar impact of gene dosage on

559 transcriptome and proteome in either LOG (enriched for procyclic promastigotes, proliferative stage)
560 or STAT (enriched for metacyclic promastigotes, infectious stage) growth phases. This is striking, as
561 the parasite featuring extensive transcriptome and proteome changes during its life cycle. For
562 example, transcriptomics studies have shown that up to 30-50% of transcripts are differentially
563 expressed between procyclic and metacyclic promastigotes [15,61]. Similarly, 10-40% of proteins are
564 differentially expressed between the parasite's promastigote and amastigote life stages [11,62].

565 A limited proportion of differential transcripts between aneuploid strains (23.6%) and the majority of
566 differential proteins (56.9%) originated from chromosomes without a change in somy, so-called
567 trans-transcripts, and trans-proteins. As we excluded genes with CNVS between strains from our
568 analysis and SNPs and INDELs were very rare, we hypothesize that the observed trans-effects could
569 result from aneuploidy, although our study does not allow to test for a causal relationship. High
570 abundances of trans-transcripts have been reported in many other aneuploidy studies on cells from
571 humans, yeast, maize, *Drosophila* and *Arabidopsis*, as well as on patients with Turner and Klinefelter
572 syndrome [46-50,63-66]. These trans-transcriptomes were typically enriched for transcription factors,
573 genes related to metabolic processes, protein metabolism, or cellular stress responses. It supports
574 the idea that the cellular system mediates the primary impact of aneuploidy by inducing
575 transcriptional changes to trans-genes. Strikingly, we did not observe this coordinated transcriptomic
576 response in *Leishmania*, with relatively low proportions of differential trans-transcripts between
577 aneuploid strains and no significant enrichment of specific functional classes amongst these. On the
578 one hand, this matches the constitutive gene abundance model of the parasite, where the
579 transcription of individual protein-coding genes can not be controlled by transcription factors. On the
580 other hand, *Leish*mania does feature substantial post-transcriptional regulation of transcript levels
581 (e.g. between life stages), so in theory, extensive regulation in response to aneuploidy could have
582 occurred at this level, but we did not observe this. Instead, we did find a surprisingly high proportion
583 of trans-proteins. It appears that trans-protein abundances are directly modulated at the translation
584 or protein-stability level, as the majority did not have underlying transcript-level changes.
585 Interestingly, these trans-proteins were significantly enriched for specific protein groups, including
586 protein metabolism-related chaperones and chaperonins, peptidases, and heat-shock proteins. This
587 is relevant as aneuploidy is known to put an extra burden on the protein-folding system and suggests
588 a similar mediation of aneuploidy-induced effects as in other Eukaryotes, but instead regulated
589 directly at the protein level. This direct modulation at protein-level (without underlying
590 transcriptional change) may in fact also be present in other Eukaryotes, but could be overshadowed

591 by the transcription factor-induced changes. For this reason, we propose *Leishmania* as an attractive
592 model to study processes of post-transcriptional modulation of protein levels in the context of
593 aneuploidy.

594 Finally, we showed that the degree of aneuploidy differences between strains matched the degree of
595 transcriptome, proteome, and differential metabolome changes. This is an important observation as
596 it suggests that aneuploidy in *Leishmania* has the capacity to drive metabolic variation, which is
597 closely linked to the phenotype. It also matches our previous observations where we linked *L.*
598 *donovani* gene copy number variants directly to changes in metabolic pathways [31]. Ultimately, it
599 supports the view that aneuploidy can be adaptive and drive the metabolic changes that the parasite
600 needs to survive in a novel environment.

601 *Conclusion*

602 In summary, our study shows that aneuploidy in *Leishmania* globally and proportionally impacts the
603 transcriptome and proteome of affected chromosomes throughout the parasite's life cycle *in vitro*. In
604 *Leishmania* strains with a closely related genetic background, the degree of these aneuploidy-
605 induced changes ultimately correlates with the degree of metabolomic difference. Similarly as in
606 other Eukaryotes, we observed dosage compensation at protein level for protein-complex subunits
607 and secreted proteins. Additionally, we found non-cytoplasmic proteins to be more compensated
608 that cytoplasmic ones. While most aneuploid Eukaryotes display extensive regulation of trans-
609 transcripts to mediate the effects of aneuploidy, we did not observe this to the same extend in
610 *Leishmania*. This suggests that the post-transcriptional mRNA regulation system of the parasite does
611 not mediate the impact of aneuploidy. Instead, *Leishmania* features a surprisingly high number of
612 trans-proteins, which are likely post-transcriptionally modulated. It thus seems that aneuploidy is
613 accompanied by trans-proteomic changes in Eukaryotes, regardless of the system of regulation. Post-
614 transcriptional modulation of trans-proteins may also be present in other Eukaryotes, but could be
615 overshadowed by the transcription factor-induced gene regulation that is absent in *Leishmania.* For
616 this reason, we believe that *Leishmania* is an attractive model to study processes of post-
617 transcriptional modulation of protein levels in the context of aneuploidy and beyond.

618

References

1 Siegel, J. J. & Amon, A. New Insights into the Troubles of Aneuploidy. *Annual review of cell and developmental biology* **28**, 189-214, doi:10.1146/annurev-cellbio-101011-155807 (2012).

2 Zhu, J., Tsai, H.-J., Gordon, M. R. & Li, R. Cellular Stress Associated with Aneuploidy. *Developmental cell* **44**, 420-431, doi:10.1016/j.devcel.2018.02.002 (2018).

3 Chen, G., Bradford, W. D., Seidel, C. W. & Li, R. Hsp90 stress potentiates rapid cellular adaptation through induction of aneuploidy. *Nature* **482**, 246, doi:10.1038/nature10795

https://www.nature.com/articles/nature10795#supplementary-information (2012).

4 Selmecki, A., Forche, A. & Berman, J. Genomic plasticity of the human fungal pathogen Candida albicans. *Eukaryotic cell* **9**, 991-1008, doi:10.1128/ec.00060-10 (2010).

5 Gresham, D. *et al.* The repertoire and dynamics of evolutionary adaptations to controlled nutrient-limited environments in yeast. *PLoS genetics* **4**, e1000303, doi:10.1371/journal.pgen.1000303 (2008).

6 Gerstein, A. C. *et al.* Polyploid titan cells produce haploid and aneuploid progeny to promote stress adaptation. *MBio* **6**, e01340-01315, doi:10.1128/mBio.01340-15 (2015).

7 Seton-Rogers, S. Fitness penalties of aneuploidy. *Nature Reviews Cancer* **17**, 142-143, doi:10.1038/nrc.2017.9 (2017).

8 Rancati, G. *et al.* Aneuploidy underlies rapid adaptive evolution of yeast cells deprived of a conserved cytokinesis motor. *Cell* **135**, 879-893, doi:10.1016/j.cell.2008.09.039 (2008).

9 Sunshine, A. B. *et al.* The Fitness Consequences of Aneuploidy Are Driven by Condition-Dependent Gene Effects. *PLOS Biology* **13**, e1002155, doi:10.1371/journal.pbio.1002155 (2015).

10 Imamura, H. *et al.* Evolutionary genomics of epidemic visceral leishmaniasis in the Indian subcontinent. *Elife* **5**, e12613 (2016).

11 Dumetz, F. *et al.* Modulation of Aneuploidy in Leishmania donovani during Adaptation to Different In Vitro and In Vivo Environments and Its Impact on Gene Expression. *mBio* **8**, e00599-00517 (2017).

12 Franssen, S. U. *et al.* Global genome diversity of the Leishmania donovani complex. *eLife* **9**, e51243, doi:10.7554/eLife.51243 (2020).

13 Sterkers, Y., Lachaud, L., Crobu, L., Bastien, P. & Pagès, M. FISH analysis reveals aneuploidy and continual generation of chromosomal mosaicism in Leishmania major. *Cell Microbiol* **13**, 274-283, doi:10.1111/j.1462-5822.2010.01534.x (2011).

14 Ivens, A. C. *et al.* The genome of the kinetoplastid parasite, Leishmania major. *Science (New York, N.Y.)* **309**, 436-442, doi:10.1126/science.1112680 (2005).

15 Cuypers, B. *et al.* Multiplexed Spliced-Leader Sequencing: A high-throughput, selective method for RNA-seq in Trypanosomatids. *Scientific Reports* **7**, 3725, doi:10.1038/s41598-017-03987-0 (2017).

16 Prieto Barja, P. *et al.* Haplotype selection as an adaptive mechanism in the protozoan pathogen Leishmania donovani. *Nature ecology & evolution*, doi:10.1038/s41559-017-0361-x (2017).

17 WHO. Proposals for the nomenclature of salivarian trypanosomes and for the maintenance of reference collections*. *Bulletin of the World Health Organization* **56**, 467-480 (1978).

18 Andrews, S. FastQC: a quality control tool for high throughput sequence data. (2010).

19 Bolger, A. M., Lohse, M. & Usadel, B. Trimmomatic: a flexible trimmer for Illumina sequence data. *Bioinformatics (Oxford, England)* **30**, 2114-2120, doi:10.1093/bioinformatics/btu170 (2014).

20 Dumetz, F. *et al.* Modulation of Aneuploidy in Leishmania donovani during Adaptation to Different In Vitro and In Vivo Environments and Its Impact on Gene Expression. *MBio* **8**, doi:10.1128/mBio.00599-17 (2017).
21 Li, H. Aligning sequence reads, clone sequences and assembly contigs with BWA-MEM. *arXiv preprint arXiv:1303.3997* (2013).
22 Li, H. A statistical framework for SNP calling, mutation discovery, association mapping and population genetical parameter estimation from sequencing data. *Bioinformatics (Oxford, England)* **27**, 2987-2993, doi:10.1093/bioinformatics/btr509 (2011).
23 Downing, T. *et al.* Whole genome sequencing of multiple Leishmania donovani clinical isolates provides insights into population structure and mechanisms of drug resistance. *Genome research* **21**, 2143-2156, doi:10.1101/gr.123430.111 (2011).
24 Anders, S., Pyl, P. T. & Huber, W. HTSeq--a Python framework to work with high-throughput sequencing data. *Bioinformatics (Oxford, England)* **31**, 166-169, doi:10.1093/bioinformatics/btu638 (2015).
25 Quinn, T. P., Erb, I., Richardson, M. F. & Crowley, T. M. Understanding sequencing data as compositions: an outlook and review. *Bioinformatics (Oxford, England)* **34**, 2870-2878, doi:10.1093/bioinformatics/bty175 (2018).
26 Tyanova, S., Temu, T. & Cox, J. The MaxQuant computational platform for mass spectrometry-based shotgun proteomics. *Nature Protocols* **11**, 2301-2319, doi:10.1038/nprot.2016.136 (2016).
27 Berg, M. *et al.* Experimental resistance to drug combinations in Leishmania donovani: metabolic and phenotypic adaptations. *Antimicrobial agents and chemotherapy* **59**, 2242-2255 (2015).
28 Berg, M. *et al.* Metabolic adaptations of Leishmania donovani in relation to differentiation, drug resistance, and drug pressure. *Mol Microbiol* **90**, 428-442, doi:10.1111/mmi.12374 (2013).
29 Benton, H. P., Want, E. J. & Ebbels, T. M. Correction of mass calibration gaps in liquid chromatography-mass spectrometry metabolomics data. *Bioinformatics (Oxford, England)* **26**, 2488-2489, doi:10.1093/bioinformatics/btq441 (2010).
30 Scheltema, R. A., Jankevics, A., Jansen, R. C., Swertz, M. A. & Breitling, R. PeakML/mzMatch: a file format, Java library, R library, and tool-chain for mass spectrometry data analysis. *Analytical chemistry* **83**, 2786-2793, doi:10.1021/ac2000994 (2011).
31 Cuypers, B. *et al.* Integrated genomic and metabolomic profiling of ISC1, an emerging Leishmania donovani population in the Indian subcontinent. *Infection, Genetics and Evolution* **62**, 170-178, doi:https://doi.org/10.1016/j.meegid.2018.04.021 (2018).
32 Prince, J. T. & Marcotte, E. M. Chromatographic alignment of ESI-LC-MS proteomics data sets by ordered bijective interpolated warping. *Anal Chem* **78**, 6140-6152, doi:10.1021/ac0605344 (2006).
33 Tautenhahn, R., Böttcher, C. & Neumann, S. Highly sensitive feature detection for high resolution LC/MS. *BMC Bioinformatics* **9**, 504, doi:10.1186/1471-2105-9-504 (2008).
34 Doyle, M. A. *et al.* LeishCyc: a biochemical pathways database for Leishmania major. *BMC Syst Biol* **3**, 57-57, doi:10.1186/1752-0509-3-57 (2009).
35 Fahy, E. *et al.* Update of the LIPID MAPS comprehensive classification system for lipids. *J Lipid Res* **50 Suppl**, S9-S14, doi:10.1194/jlr.R800095-JLR200 (2009).
36 Kanehisa, M., Furumichi, M., Tanabe, M., Sato, Y. & Morishima, K. KEGG: new perspectives on genomes, pathways, diseases and drugs. *Nucleic acids research* **45**, D353-d361, doi:10.1093/nar/gkw1092 (2017).
37 Wishart, D. S. *et al.* HMDB 4.0: the human metabolome database for 2018. *Nucleic acids research* **46**, D608-d617, doi:10.1093/nar/gkx1089 (2018).

38 Tihon, E. *et al.* Genomic analysis of Isometamidium Chloride resistance in Trypanosoma congolense. *International Journal for Parasitology: Drugs and Drug Resistance* **7**, 350-361, doi:https://doi.org/10.1016/j.ijpddr.2017.10.002 (2017).
39 Wickham, H. *ggplot2: Elegant Graphics for Data Analysis.* (Springer-Verlag New York, 2016).
40 Krzywinski, M. I. *et al.* Circos: An information aesthetic for comparative genomics. *Genome research*, doi:10.1101/gr.092759.109 (2009).
41 Hunter, J. D. Matplotlib: A 2D Graphics Environment. *Computing in Science & Engineering* **9**, 90-95, doi:10.1109/MCSE.2007.55 (2007).
42 Virtanen, P. *et al.* SciPy 1.0: fundamental algorithms for scientific computing in Python. *Nature Methods* **17**, 261-272, doi:10.1038/s41592-019-0686-2 (2020).
43 Imamura, H. *et al.* Evolutionary genomics of epidemic visceral leishmaniasis in the Indian subcontinent. *Elife* **5**, doi:10.7554/eLife.12613 (2016).
44 Dumetz, F. *et al.* Molecular Preadaptation to Antimony Resistance in Leishmania donovani on the Indian Subcontinent. *mSphere* **3**, e00548-00517, doi:10.1128/mSphere.00548-17 (2018).
45 Laffitte, M.-C. N. *et al.* Formation of Linear Amplicons with Inverted Duplications in Leishmania Requires the MRE11 Nuclease. *PLoS genetics* **10**, e1004805, doi:10.1371/journal.pgen.1004805 (2014).
46 Hwang, S. *et al.* Consequences of aneuploidy in human fibroblasts with trisomy 21. *Proceedings of the National Academy of Sciences* **118**, e2014723118, doi:10.1073/pnas.2014723118 (2021).
47 Torres, E. M. *et al.* Effects of Aneuploidy on Cellular Physiology and Cell Division in Haploid Yeast. *Science* **317**, 916-924, doi:10.1126/science.1142210 (2007).
48 Makarevitch, I., Phillips, R. L. & Springer, N. M. Profiling expression changes caused by a segmental aneuploid in maize. *BMC Genomics* **9**, 7, doi:10.1186/1471-2164-9-7 (2008).
49 Huettel, B., Kreil, D. P., Matzke, M. & Matzke, A. J. M. Effects of Aneuploidy on Genome Structure, Expression, and Interphase Organization in Arabidopsis thaliana. *PLoS genetics* **4**, e1000226, doi:10.1371/journal.pgen.1000226 (2008).
50 Sheltzer, J. M., Torres, E. M., Dunham, M. J. & Amon, A. Transcriptional consequences of aneuploidy. *Proc Natl Acad Sci U S A* **109**, 12644-12649, doi:10.1073/pnas.1209227109 (2012).
51 Berg, M. *et al.* Metabolic adaptations of Leishmania donovani in relation to differentiation, drug resistance, and drug pressure. *Molecular Microbiology* **90**, 428-442, doi:10.1111/mmi.12374 (2013).
52 Iantorno, S. A. *et al.* Gene Expression in Leishmania Is Regulated Predominantly by Gene Dosage. *mBio* **8**, doi:10.1128/mBio.01393-17 (2017).
53 Dephoure, N. *et al.* Quantitative proteomic analysis reveals posttranslational responses to aneuploidy in yeast. *eLife* **3**, e03023, doi:10.7554/eLife.03023 (2014).
54 Stingele, S. *et al.* Global analysis of genome, transcriptome and proteome reveals the response to aneuploidy in human cells. *Mol Syst Biol* **8**, 608, doi:10.1038/msb.2012.40 (2012).
55 McShane, E. *et al.* Kinetic Analysis of Protein Stability Reveals Age-Dependent Degradation. *Cell* **167**, 803-815.e821, doi:10.1016/j.cell.2016.09.015 (2016).
56 Schukken, K. M. & Sheltzer, J. M. Extensive protein dosage compensation in aneuploid human cancers. *bioRxiv*, 2021.2006.2018.449005, doi:10.1101/2021.06.18.449005 (2021).
57 Veitia, R. A., Bottani, S. & Birchler, J. A. Cellular reactions to gene dosage imbalance: genomic, transcriptomic and proteomic effects. *Trends in Genetics* **24**, 390-397, doi:10.1016/j.tig.2008.05.005 (2008).
58 Gilchrist, C. & Stelkens, R. Aneuploidy in yeast: Segregation error or adaptation mechanism? *Yeast* **36**, 525-539, doi:10.1002/yea.3427 (2019).

59 Robinson, D., Place, M., Hose, J., Jochem, A. & Gasch, A. P. Natural variation in the consequences of gene overexpression and its implications for evolutionary trajectories. *eLife* **10**, e70564, doi:10.7554/eLife.70564 (2021).
60 Larrimore, K. E., Barattin-Voynova, N. S., Reid, D. W. & Ng, D. T. W. Aneuploidy-induced proteotoxic stress can be effectively tolerated without dosage compensation, genetic mutations, or stress responses. *BMC Biology* **18**, 117, doi:10.1186/s12915-020-00852-x (2020).
61 Dillon, L. A. L. *et al.* Transcriptomic profiling of gene expression and RNA processing during Leishmania major differentiation. *Nucleic acids research* **43**, 6799-6813, doi:10.1093/nar/gkv656 (2015).
62 Lynn, M. A., Marr, A. K. & McMaster, W. R. Differential quantitative proteomic profiling of Leishmania infantum and Leishmania mexicana density gradient separated membranous fractions. *J Proteomics* **82**, 179-192, doi:10.1016/j.jprot.2013.02.010 (2013).
63 Sun, L. *et al.* Dosage compensation and inverse effects in triple X metafemales of *Drosophila*. *Proceedings of the National Academy of Sciences* **110**, 7383-7388, doi:doi:10.1073/pnas.1305638110 (2013).
64 Hou, J. *et al.* Global impacts of chromosomal imbalance on gene expression in Arabidopsis and other taxa. *Proc Natl Acad Sci U S A* **115**, E11321-e11330, doi:10.1073/pnas.1807796115 (2018).
65 Raznahan, A. *et al.* Sex-chromosome dosage effects on gene expression in humans. *Proceedings of the National Academy of Sciences* **115**, 7398-7403, doi:doi:10.1073/pnas.1802889115 (2018).
66 Zhang, X. *et al.* Integrated functional genomic analyses of Klinefelter and Turner syndromes reveal global network effects of altered X chromosome dosage. *Proceedings of the National Academy of Sciences* **117**, 4864-4873, doi:doi:10.1073/pnas.1910003117 (2020).

Funding

This work was supported by the Research Foundation Flanders [11O1614N to B.C.]; the Interuniversity Attraction Poles Program of Belgian Science Policy [P7/41 to JC.D.], the InBev Baillet-Latour foundation and the Department of Economy, Science and Innovation in Flanders [ITM-SOFIB, SINGLE to JC.D.]

Acknowledgements

We thank the Center of Medical Genetics at the University of Antwerp for hosting the NGS facility on which our RNA-Seq experiments were performed. The computational resources used for this work were provided by the VSC (Flemish Supercomputer Center) at the University of Antwerp.

Data Availability Statement

The raw genomic and transcriptomic data in this study is available at the NCBI Sequence Read Archive (SRA) under the accession code: PRJNA762444. Raw proteomic data has been submitted to the PRIDE database under reference 1-20210911-141001. Raw metabolomic data was submitted to the MetaboLights database under accession code MTBLS1612.

Conflict of Interest

The authors declare that they have no conflict of interest.

Supplementary Tables

Supplementary Table S1.A

Detailed description of the *L. donovani* isolates used in this study.

Supplementary Table S1.B

Number of total SNPs, non-synonmous SNPs and homozygous non-synonymous SNPs between any pair of *L. donovani* strains in this study.

Supplementary Table S1.C

Sequencing quality and mapping statistics of all 6 sequenced *L. donovani* genomes in this study.

Supplementary Table S1.D

Sequencing quality and mapping statistics of all sequenced *L. donovani* transcriptomes in this study.

Supplementary Table S1.E

Dosage compensation model data, coefficients and *p*-values.

Supplementary Table S1.F

Summary of all cis- and trans- transcripts and proteins of all possible pairwise comparisons between the 6 *L. donovani* strains in this study.

Supplementary Table S1.G

Pooled trans-transcripts from all possible pairwise comparisons between the 6 *L. donovani* strains in this study.

Supplementary Table S1.H

Pooled trans-proteins from all possible pairwise comparisons between the 6 *L. donovani* strains in this study.

Supplementary Table S1. I

Upregulated metacyclogenis markers in STAT growth phase. Output generated by DESeq2.

Supplementary Table S2

Structure (Somy and local CNVs) of all sequenced *L. donovani* genomes in this study.

Supplementary Table S3

Differential RNA abundance analyses of the different biological comparisons made in this study.

833 **Supplementary Table S4**

834 Detailed statistics about all proteins detected in this study. Output generated by MaxQuant.

835 **Supplementary Table S5**

836 Detailed statistics about all metabolites detected in this study.

837 Supplementary Figures

838 **Supplementary Figure S1.A & S1.B**

839 Comparative Circos plot between BPK173 and BPK288 (S1.A) and between BHU575 and BPK282
840 (S1.B), showing their relative (expressed in fold change) gene dosage (blue), transcript abundance
841 (orange), and protein abundance (purple) across the 36 *L. donovani* chromosomes.